SSC-168

Superconducting Super Collider Laboratory

SSC-168

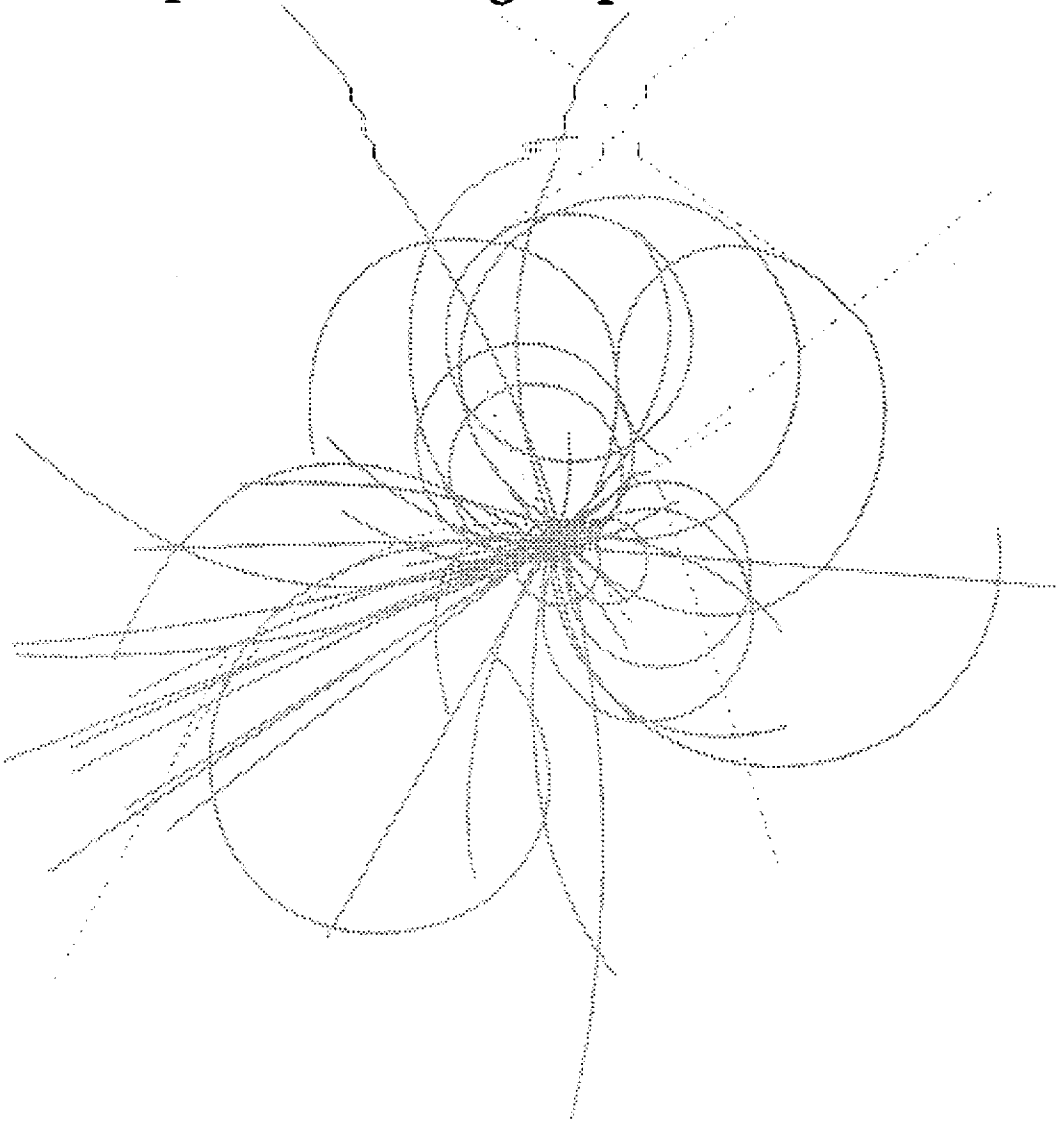

Allowable Stress in the SSC Beam Tube During a Quench

K.-Y. Ng and J. Peterson
SSC Central Design Group

March 1988

SSC-168

ALLOWABLE STRESS IN THE SSC BEAM TUBE DURING A QUENCH

King-Yuen Ng
SSC Central Design Group*
c/o Lawrence Berkeley Laboratory, Berkeley, CA 94720
and
Fermi National Accelerator Laboratory, Batavia, IL 60510

and

Jack Peterson
SSC Central Design Group*
c/o Lawrence Berkeley Laboratory, Berkeley, CA 94720

March 1988

*Operated by Universities Research Association for the U. S. Department of Energy

I. INTRODUCTION

In order to minimize transverse resistive wall instability, the SSC beam tube has been designed with a 2-mil layer of inside copper coating. This is because the conductivity of copper at helium temperature can be 300 to 3000 times larger than that of stainless steel or Nitronic 40. Since this instability is a long-wavelength effect, a thicker copper layer would be more beneficial. However, a thick copper layer is bad with respect to the possible inelastic deformation of the beam tube during a quench of the superconducting magnet. The eddy current induced in the beam tube resides mostly in the copper layer and is directly proportional to the layer thickness t_1. Being immersed in a vertical dipole magnetic flux density B, the copper layer will exert a horizontal outward Lorentz pressure on the beam tube, deforming it into an approximate ellipse. The bigger the Lorentz deformation, the easier it is for the partially vaporized helium to further deform the beam tube.

The Lorentz pressure

$$P_L(\varphi) = P_m \sin\varphi \ , \tag{1.1}$$

varies sinusoidally with the polar angle φ as illustrated in Fig. 1a, and P_m is the pressure at the equator ($\varphi = \pi/2$) given by

$$P_m = \sigma_1 |B\dot{B}| t_1 R \ . \tag{1.2}$$

For completeness, Eqs. (1.1) and (1.2) are derived in Appendix A. Obviously, the conductivity of copper σ_1, the dipole magnetic flux density B, and its time rate of change $\dot{B}$ are all time dependent during the quench, but the maximum is implied in Eq. (1.2). For a copper layer of 2 mils, P_m can be as big as ~ 100 psi. Equation (1.2) is in mks units. If B is in tesla, $\dot{B}$ in tesla/sec, R and t_1 in m, and σ_1 in $(\Omega\text{-m})^{-1}$, then the pressure P_m will be in newton/m^2. To convert to psi or atmospheres, the factors 1 newton/m^2 $= 1.45 \times 10^{-4}$ psi and 1 atm $= 14.68$ psi should be used.

The purpose of this article is to compute the helium pressure required to distort the beam tube beyond its elastic limit when a maximum equatorial Lorentz pressure P_m is applied. There are two reasons that we talk about the elastic limit here instead of the crushing of the beam tube. First, the computation is much simpler because Hooke's law can be applied approximately. Second, slightly beyond the elastic limit of most materials comes the yield point, beyond which the material becomes plastic and would be permanently deformed. Thus it is convenient and conservative to stay below the elastic limit. Since the yield points of materials are more easily obtained from tables than the elastic limits, we will take the yield point as the approximate elastic limit in our discussions below.

This article is written for physicists and is designed to be self-contained. All the basic theories used will be described, and all the formulas used will be derived.

Therefore, the reader is not required to have any prerequisite knowledge of strength of materials. Most of the materials are taken from the text by Timoshenko.[1]

In Section II, we derive the basic equation describing the elastic deformation of a body under stress and the conditions under which that body will be deformed permanently. In Section III, we review the theory of buckling which gives another limitation to the applied stress. In Section IV, the deformation of the beam tube under the Lorentz pressure of Eq. (1.1) is computed. In Section V, a uniform helium pressure is introduced outside the beam tube. A further deformation of the tube is computed, and the helium pressure required to deform the tube beyond the elastic limit is derived. Finally in Section VI, the failure limitations of the keys on the outside of the bore tube due to a nonuniform copper layer are discussed.

II. THE BASIC DEFORMATION EQUATION

Consider a uniform massive beam supported at both ends as shown in Fig. 2a. Due to its own weight, the beam will be bent. Consider the section AB in Fig. 2b and study the forces acting in the cross section B. There are a tensile force T parallel to the beam and a shearing force S perpendicular to the beam as a result of the imbalance of the weight of the section AB and the reaction at A. We observe that the moment of these forces are in general not balanced also. Therefore, there must be a couple at the cross section B, which is known as the *bending moment* at B. Physically, this bending moment arises from the compression at the upper surface and elongation at the lower surface of the beam that has been bent. It is the pressing in at the top and pushing out at the bottom that generates this moment.

The neutral axis in the beam is the line inside the beam where there is no compression or elongation. We denote this the x-direction and consider an infinitesimal section of length dx as in Fig. 2c. The y-axis is perpendicular to the x-axis and is pointing downward. The z-axis is the other lateral direction. At a distance y from the neutral axis, the axial extension is Δ corresponding to an axial strain $\epsilon_x(y)$ in the x-direction equal to

$$\epsilon_x(y) = \frac{\Delta}{dx} = \frac{y}{\rho_{xy}} , \tag{2.1}$$

where ρ_{xy} is the local radius of curvature of the x-axis in the y direction. We will be using this subscript convention for the radius of curvature ρ_{xy} and the bending moment M_{xy} below, where the first subscript denotes the axis to be bent and the second subscript denotes the direction of bending. The axial stress at y due to the bending is therefore

$$\sigma_x(y) = E\epsilon_x(y) = \frac{Ey}{\rho_{xy}} , \tag{2.2}$$

where E is the Young's modulus of elasticity for the beam material, and Hooke's law is assumed. This bending couple or moment does not contribute any net force along the beam direction because we have grouped all possible net forces at cross section B into the tensile force T and the shearing force S. The integral of Eq. (2.2) across the beam from top to bottom should therefore vanish. This indicates that the neutral axis is at the center of the beam. The bending moment M_{xy} that causes bending of the x-axis in the y direction can now be computed by multiplying $\sigma_x(y)$ by y and integrating over the cross section of the beam,

$$M_{xy} = \frac{EI_x}{\rho_{xy}} , \tag{2.3}$$

where the *moment of inertia*

$$I_x = \int y^2 dA \tag{2.4}$$

is defined as the integral of the second moment over the cross section normal to the x-direction. Equation (2.3) holds for every cross section along the beam and is the basic equation describing the beam deformation. There should be a sign convention for M_{xy} and ρ_{xy} which we have not specified here. We just infer to the sign through physical intuition.

For a rectangular beam of height h and width ℓ, the moment of inertia can be easily found to be

$$I_x = \frac{h^3 \ell}{12} . \tag{2.5}$$

As the beam is compressed at the top and stretched at the bottom, the lateral width in the z-direction will naturally be stretched at the top and compressed at the bottom so that the cross section has a shape as depicted in Fig. 2d. Therefore, there is stress σ_z and bending moment M_{zy} also. The beam is bent in the lateral direction and a radius of curvature ρ_{zy} can be introduced. Now the strains in both the x and the z directions are given by equations like Eq. (2.1)

$$\begin{cases} \epsilon_x = \dfrac{y}{\rho_{xy}} , \\ \\ \epsilon_z = -\dfrac{y}{\rho_{zy}} . \end{cases} \tag{2.6}$$

However, there is no bending of the y-axis and therefore no bending moment M_{yx} or M_{yz}. In other words, there is no tensile stress σ_y in the y-direction.

To describe the picture, the convenient Poisson's ratio

$$\mu = \frac{\text{unit lateral contraction}}{\text{unit axial elongation}} \tag{2.7}$$

is defined, when the body is subjected to axial stress only. If a body is compressed in one direction, it is unlikely that the volume of the body expands. This supposition implies that the Poisson's ratio should be less than 1/2. Poisson determined this ratio analytically by using molecular theory of the structure of material. For materials which have the same elastic properties in all directions, he found $\mu = 1/4$. For an infinitesimal cube of the beam, taking these lateral contractions into account, the linear Hooke's law is modified generally to

$$\begin{pmatrix} \epsilon_x \\ \epsilon_y \\ \epsilon_z \end{pmatrix} = \begin{pmatrix} 1 & -\mu & -\mu \\ -\mu & 1 & -\mu \\ -\mu & -\mu & 1 \end{pmatrix} \begin{pmatrix} \dfrac{\sigma_x}{E} \\ \dfrac{\sigma_y}{E} \\ \dfrac{\sigma_z}{E} \end{pmatrix} . \tag{2.8}$$

Our problem simplifies because there is no stress in the y-direction ($\sigma_y = 0$); but there is strain in the y-direction,

$$\epsilon_y = -\mu \frac{\sigma_x}{E} - \mu \frac{\sigma_z}{E} . \tag{2.9}$$

From Eqs. (2.6) and (2.8), we obtain

$$\begin{cases} \sigma_x = \dfrac{Ey}{1-\mu^2} \left(\dfrac{1}{\rho_{xy}} - \dfrac{\mu}{\rho_{zy}} \right) , \\ \sigma_z = \dfrac{Ey}{1-\mu^2} \left(-\dfrac{1}{\rho_{zy}} + \dfrac{\mu}{\rho_{xy}} \right) . \end{cases} \tag{2.10}$$

The respective bending moments are

$$\begin{cases} M_{xy} = \dfrac{EI_x}{1-\mu^2} \left(\dfrac{1}{\rho_{xy}} - \dfrac{\mu}{\rho_{zy}} \right) , \\ M_{zy} = \dfrac{EI_z}{1-\mu^2} \left(-\dfrac{1}{\rho_{zy}} + \dfrac{\mu}{\rho_{xy}} \right) , \end{cases} \tag{2.11}$$

where I_z is the moment of inertia defined similar to Eq. (2.4) but with the integration over an area normal to the z-direction. These are the two equations governing the deformations in both the axial and lateral directions.

However, in the case of a plate where the z-dimension ℓ is very big (or the case of a long tube where the length corresponds to the z-direction), the lateral deformation

in the y-z cross section (Fig. 2d) will not be possible, or $1/\rho_{zy} = 0$. Then we get

$$M_{xy} = \frac{EI_x}{\rho_{xy}(1-\mu^2)} , \tag{2.12}$$

which is exactly the same as Eq. (2.3) if we make the substitution

$$E \rightarrow E' = \frac{E}{1-\mu^2} . \tag{2.13}$$

This is expected because the restriction in a change of the lateral direction will definitely increases the stress in the axial direction. Since we are not interested in the lateral direction, we shall drop all the subscripts in the following unless there is ambiguity.

The factor $1/\rho$ is the curvature of the bent beam for the case when the beam is originally straight. For a beam that is curved to start with, $1/\rho$ should be interpreted as the *change in curvature*.

Suppose the beam originally has a radius of curvature ρ_0 at a point, we can write

$$\frac{1}{\rho_0} = \frac{d\varphi}{ds} , \tag{2.14}$$

where ds is the length of the beam AB covered by an infinitesimal angle $d\varphi$ as shown in Fig. 3. The beam is now bent so that AB becomes $A'B'$. The new curvature is now given by

$$\frac{1}{\rho'} = \frac{d\varphi - \left(\left.\frac{du}{ds}\right|_{B'} - \left.\frac{du}{ds}\right|_{A'} \right)}{ds + \Delta ds} , \tag{2.15}$$

where u is the radial displacement at A' or B' and

$$\Delta ds = \frac{u}{\rho_0} ds \tag{2.16}$$

is the increase in arc length from AB to $A'B'$. So far we have been keeping only first order terms in the beam deformation u. The change in curvature is

$$\frac{1}{\rho'} - \frac{1}{\rho_0} = -\frac{d^2u}{ds^2} - \frac{u}{\rho_0} , \tag{2.17}$$

which when substituted for $1/\rho$ in Eq. (2.3) leads to a linearized basic equation for bent beam,

$$EI\left(\frac{d^2u}{d\varphi^2} + u\right) = -M\rho_0^2 . \tag{2.18}$$

We want to remark that Eq. (2.18) has been linearized. Also in both Eqs. (2.3) and (2.18), the deformations due to tensile forces and shearing forces have not been included. For a tube of thickness h and radius R, these deformations are about $(h/R)^2$ times smaller than the deformations due to bending moments.

The deformed beam will return to its original shape once the stress is relieved if we are in the strain-stress proportional region where Hooke's law holds (or more generally in the elastic region). However, when the stress passes the yield point σ_{yp}, this is no longer true. The beam will not return to its original shape and is permanently deformed. Sometimes the material goes plastic and even collapses. In this article, we confine our study to within the elastic limit where Hooke's law holds approximately. Also the yield point will be taken as an approximation for the elastic limit. With a bending moment M, the stress is a maximum at the upper or lower edge of the beam where the compression or stretching is greatest. Therefore,

$$\sigma_{\max} = \frac{E'h}{2|\rho|} \ . \tag{2.19}$$

Eliminating ρ with Eq. (2.12) and using the explicit expression (2.5) for the moment of inertia, we obtain the maximum stress due to a bending moment M,

$$\sigma_{\max} = \frac{h|M|}{2I} = \frac{6|M|}{h^2\ell} \ . \tag{2.20}$$

The total stress in the direction of the beam must also include the tensile stress T/A where A is the beam cross-sectional area. Thus, to prevent permanent deformation, we must require

$$\frac{|T|}{A} + \frac{6|M|}{h^2\ell} < \sigma_{yp} \ . \tag{2.21}$$

In the direction perpendicular to the beam, there is a shear-stress yield point τ_{yp} also. Thus in addition to criterion (2.21), we also require

$$\frac{|S|}{A} < \tau_{yp} \ . \tag{2.22}$$

A shear elastic modulus G can be defined as the ratio of the shearing stress to the shearing strain. The shearing of a rectangle into a parallelogram can be described by the elongation of one diagonal and the contraction of the other. Therefore the shear modulus is related to the tensile elastic modulus E, and it is easy to show that[1]

$$G = \frac{E}{2(1+\mu)} \ . \tag{2.23}$$

Experimental observations indicate that

$$\tau_{yp} \approx \frac{1}{2}\sigma_{yp} \ . \tag{2.24}$$

It appears that Eq. (2.24) follows from Eq. (2.23), but in fact they are not related because the mechanism of shear failure can be quite different from the mechanism of stress failure.

Some remarks are in order. Consider a rod of cross sectional area A is stretched by a tensile force T. Because of lateral contractions, the tensile stress is, according to Eq. (2.7),

$$\sigma = \frac{T}{A(1-\mu\sigma/E)^2} \ . \tag{2.25}$$

Denoting by $\sigma' = T/A$ the approximate stress with the lateral contractions neglected, Eq. (2.25) can be solved by perturbation to give

$$\sigma = \sigma'\left(1 + 2\mu\frac{\sigma'}{E}\right) + \cdots \ . \tag{2.26}$$

If the tensile force is a compression, the sign before μ should be changed. Since σ'/E is roughly the strain, which is small, it is usually neglected so that we need not distinguish between σ and σ'. Also the elongation yield point should in principle be different from the compression yield point. But experimental measurements show that they are roughly the same. These approximations have been made in developing Eqs. (2.21) and (2.22).

III. THEORY OF ELASTIC BUCKLING

Consider a rod of length ℓ standing vertically on the floor. We apply a vertical force F on its top and increase F until the rod buckles with a horizontal displacement $y = \delta$ at its center (Fig. 4a). Taking the x-axis as vertical, the curvature of the buckled rod at a point (x, y) on the rod is

$$\frac{1}{\rho} \approx -\frac{d^2y}{dx^2} \ . \tag{3.1}$$

The bending moment there

$$M = Fy \tag{3.2}$$

can be obtained easily by considering the section from the floor up to (x, y) and taking moment about the point (x, y). Here, the shearing force which is of order δ/ℓ of F

and has been neglected. The basic equation (2.3) describing the beam deformation becomes

$$-EI\frac{d^2y}{dx^2} = Fy \ , \tag{3.3}$$

or

$$\frac{d^2y}{dx^2} + c^2y = 0 \ , \tag{3.4}$$

with

$$c^2 = \frac{F}{EI} \ . \tag{3.5}$$

The Poisson ratio dependency has been dropped for simplicity. The solution must satisfy the following three sets of boundary conditions:

$$\begin{aligned} &(1) \qquad y = 0 \quad \text{at } x = 0 \text{ and } \ell \ , \\ &(2) \qquad y = \delta \quad \text{at } x = \frac{\ell}{2} \ , \\ &(3) \qquad y' = 0 \quad \text{at } x = \frac{\ell}{2} \ . \end{aligned} \tag{3.6}$$

However, the deformation equation is of only second order; thus a solution is not always possible. Imposing boundary conditions (2) and (3), the solution is

$$y = \delta \cos c\left(\frac{\ell}{2} - x\right) \ . \tag{3.7}$$

Then in order to satisfy boundary condition (1), we need to set

$$\frac{c\ell}{2} = \frac{\pi}{2}, \ \frac{3\pi}{2}, \cdots \ , \tag{3.8}$$

so that the force becomes

$$F_c = \frac{\pi^2 EI}{\ell^2}, \ \frac{9\pi^2 EI}{\ell^2}, \cdots \ . \tag{3.9}$$

The solution says that to buckle the rod and maintain a finite horizontal displacement δ midway, a force of $F_c = \pi^2 EI/\ell^2$ is needed. Below that a stable deformation will not occur. The next solution is the buckling of the rod into a shape with two nodes. This solution requires a force that is nine times bigger and is in general of no physical interest because the rod will usually reach its yield point much earlier.

Our solution appears unphysical because the applied force is quantized, and we cannot increase it even slightly bigger than F_c. Also the amount of buckling δ is independent of the applied force.

These apparent unphysical effects occur because we have been assuming the height of the rod to be ℓ although it is bent. The error is second order in δ/ℓ. If we want to correct for this, we need to include the second order terms for the curvature. In fact, if we use the full formula for the curvature

$$\frac{1}{\rho} = \frac{\dfrac{d^2y}{dx^2}}{\left[1+\left(\dfrac{dy}{dx}\right)^2\right]^{3/2}} , \tag{3.10}$$

the exact solution of the deformation equation gives a buckling of[2]

$$\delta = \frac{2\sqrt{2}\ell}{\pi}\sqrt{\frac{F}{F_c}-1}\left[1-\frac{1}{8}\left(\frac{F}{F_c}-1\right)\right] \tag{3.11}$$

for $F > F_c$ and $\delta = 0$ for $F < F_c$. The solution is plotted in Fig. 4b. We see that the increase in deformation per unit increase in the applied force is

$$\frac{d\delta}{dF} = \frac{\sqrt{2}\ell}{\pi}\frac{1-\dfrac{3}{8}\left(\dfrac{F}{F_c}-1\right)}{\sqrt{\dfrac{F}{F_c}-1}} , \tag{3.12}$$

which is very big when F is just bigger than F_c (and is actually infinite at F_c). Therefore, as soon as F passes F_c, a slight increase in the applied force will cause an enormous increase in the deformation. Thus the elastic limit will usually be reached when F exceeds F_c slightly. For this reason we call F_c the critical buckling force. To safeguard the stability of the rod against collapse, we always require the applied force to be less than F_c.

IV. DEFORMATION DUE TO LORENTZ PRESSURE

During a quench, the maximum horizontal outward Lorentz force acting at polar angle φ for a length ℓ of the beam tube is (Fig. 1a)

$$dF(\varphi) = P_m R\ell \sin\varphi d\varphi , \tag{4.1}$$

where the maximum equatorial Lorentz pressure P_m is given in Eq. (1.2) and R is the beam tube radius. The details are given in Appendix A. The total horizontal Lorentz force on each half of the beam tube is therefore

$$F_t = 2P_m R\ell . \tag{4.2}$$

Take the segment VC. At the cross section V or $\varphi = 0$, there is a tensile force $F_t/2$. Taking moment about C, the bending moment at C is (Fig. 1b)

$$M_\varphi = M_0 - \int_0^\varphi \frac{1}{2} F_t \sin\theta R(\cos\theta - \cos\varphi) d\theta + \frac{1}{2} F_t R(1 - \cos\varphi) \ , \tag{4.3}$$

where M_0 is the bending moment supporting the segment VC at V. We can rewrite Eq. (4.3) as

$$M_\varphi = -\frac{1}{8} F_t R \cos 2\varphi + M_0' \ , \tag{4.4}$$

where $M_0' = M_0 + F_t R/8$. The deviation from the circular cross section $u(\varphi)$ satisfies the deformation equation (2.18),

$$E'I \left(\frac{d^2 u}{d\varphi^2} + u \right) = \frac{1}{8} F_t R^3 \cos 2\varphi - M_0' R^2 \ , \tag{4.5}$$

where we use the Poisson modified modulus $E' = E/(1-\mu^2)$ because we are studying a *long* tube. We expect the deformed cross section to be symmetric with respect to the vertical and horizontal axes. The only solution is

$$u = -\frac{F_t R^3}{24 E' I} \cos 2\varphi \ , \tag{4.6}$$

with $M_0' = 0$. That is, the cross section has an elliptical shape

$$r = R + u_0 \cos 2\varphi \ , \qquad u_0 = -\frac{F_t R^3}{24 E' I} \ . \tag{4.7}$$

In computing M_φ, we have assumed a circular cross section instead of the actual deformed ellipse-like cross section. The error is an order u_0/R smaller. These extra terms should be deleted because the deformation equation (2.18) has been linearized.

The elongation at $\varphi = \pi/2$ and flattening at $\varphi = 0$ as well as the bending moment at $\varphi = 0$ can also be obtained by variations of the energy of deformation without actually solving the deformation equation. The details are given in the Appendix B for the interested readers.

We next compute the maximum stress in the deformed tube. The maximum stress due to bending moment is given by Eq. (2.20) or

$$\sigma_{\max}|_{\text{moment}} = \frac{3}{2} \left(\frac{R}{h} \right)^2 P_m \cos 2\varphi \ , \tag{4.8}$$

which attains the largest value at the point H ($\varphi = \pi/2$), where

$$\sigma_H = \frac{3}{2} \left(\frac{R}{h} \right)^2 P_m \ . \tag{4.9}$$

At point V, there is the extra tensile stress $F_t/2h\ell$; or

$$\sigma_V = \frac{R}{h}P_m + \frac{3}{2}\left(\frac{R}{h}\right)^2 P_m \ . \tag{4.10}$$

Thus, point V is subject to higher stress than point H. Equating σ_V to the tensile yield-point stress σ_{yp}, we obtain the yield Lorentz pressure

$$(P_m)_{yp} = \frac{\sigma_{yp}}{\frac{R}{h}\left(1 + \frac{3R}{2h}\right)} \ . \tag{4.11}$$

The beam tube is under a shearing force of

$$S_L = P_m R\ell \cos\varphi \sin\varphi \tag{4.12}$$

due to the non-cylindrically distributed Lorentz pressure. A yield will occur first at the $\varphi = \pi/4$ points when

$$P_m = \frac{2h}{R}\tau_{yp} \ . \tag{4.13}$$

Considering the fact that $\tau_{yp} \approx \sigma_{yp}/2$, we see that this yield Lorentz pressure in shear is always bigger than the yield in tension given by Eq. (4.11) so it does not bother us at all.

The SSC has a beam tube radius $R = 1.66$ cm and wall thickness $h = 0.10$ cm. Equating σ_V to the yield-point stress σ_{yp} of Nitronic 40 at various temperatures and taking a Poisson ratio of $\mu = 0.287$, we can solve for the corresponding yield-point equatorial Lorentz pressures. The results are listed in Table I.

Temperature K	Yield-point Stress σ_{yp} (psi)	Yield Pressure P_m (psi)
296.8	58,000	134.9
194.1	87,000	202.4
77.4	150,000	348.9
20.0	175,000	407.0
4.0	196,000	455.9

Table I: Yield equatorial Lorentz pressure for Nitronic 40 at different temperatures

V. ADDITIONAL STRESS DUE TO HELIUM PRESSURE

During a quench, the liquid helium outside the beam tube will be partially vaporized due to the heat generated by the eddy current in the copper coating and superconducting coils. As a result, there will be a significant increase in helium pressure. Since the beam tube will be deformed by the horizontal Lorentz force, the helium pressure required to buckle the tube will be reduced.

With only helium pressure acting on a circular beam tube, the forces are radially symmetric, so that no bending moment is produced and there will be no deformation below the critical buckling pressure. Therefore, we need to compute the bending moment of the actually deformed beam tube. On the other hand, the first-order contribution of the Lorentz force can be obtained from the undeformed beam tube because the Lorentz force is not radially symmetric.

Figure 5a shows the deformed ellipse-like cross section together with the undeformed circular cross section. Because of symmetry, there are four points A, B, C, and D where the deformation is zero and the radius of curvature is unchanged. Thus the bending moments there are exactly zero. However, at each of those points there is a tensile force and a shearing force due to the helium pressure p. Take the segment AB. The horizontal forces acting at the ends A and B against the helium pressure are $p\ell R\cos\alpha$, where $2R\cos\alpha$ is the distance between A and B and ℓ is the length of tube considered. The angle α is $\pi/2$ if the deformed cross section is exactly elliptical. Similarly, for the segment AD, there are vertical forces $p\ell R\sin\alpha$ acting at A and D. Therefore, the net force acting at A on the segment AB is $F = pR\ell$ and is tangential to the undeformed circle instead of the ellipse-like boundary. This implies that shearing forces have been included in the computation. A similar force $F = pR\ell$ acts at B.

We now consider the segment AA'. Taking moment about A', we obtain the bending moment at A' (Fig. 5b)

$$M_{A'} = -pR\ell\overline{AG} + \frac{1}{2}p\ell\overline{AA'}^2 - \frac{1}{4}\ell R^2 P_m \cos 2\varphi \ , \tag{5.1}$$

where the first term on the right is due to the force F at A, the second term is due to the helium pressure acting on the arc AA', and the third term represents the Lorentz pressure given in Eq. (4.4). Using the cosine law

$$\begin{aligned} \overline{AA'}^2 &= \overline{OA}^2 + \overline{OA'}^2 - 2\overline{OG}\,\overline{OA} \\ &= \overline{OA'}^2 - \overline{OA}^2 + 2\overline{AG}\,\overline{OA} \ , \end{aligned} \tag{5.2}$$

and keeping only terms of first order in deformation, it is easy to show that

$$M_{A'} = pR\ell u - \frac{1}{4}\ell R^2 P_m \cos 2\varphi \ , \tag{5.3}$$

where $u = \overline{OA'} - R$ is the radial deformation at A'. The deformation equation can now be written as

$$E'I\left(\frac{d^2u}{d\varphi^2} + u\right) = -R^2\left(pR\ell u - \frac{1}{4}\ell R^2 P_m \cos 2\varphi\right) . \tag{5.4}$$

In Section IV, we have already solved the deformation due to Lorentz pressure,

$$E'I\left(\frac{d^2u_1}{d\varphi^2} + u_1\right) = \frac{1}{4}\ell R^4 P_m \cos 2\varphi , \tag{5.5}$$

where

$$u_1 = -\frac{\ell R^4 P_m}{12E'I}\cos 2\varphi . \tag{5.6}$$

If we *define* u_1 as the deformation due to the Lorentz pressure and $u_2 = u - u_1$ as the deformation due to the helium pressure, u_2 satisfies

$$E'I\left(\frac{d^2u_2}{d\varphi^2} + u_2\right) = -pR^3\ell(u_1 + u_2) . \tag{5.7}$$

With the help of Eq. (5.6), Eq. (5.7) can be solved easily to give

$$u_2 = \frac{pu_1}{p_c - p} , \tag{5.8}$$

where

$$p_c = \frac{3E'I}{R^3\ell} = \frac{Eh^3}{4(1-\mu^2)R^3} \tag{5.9}$$

is the critical buckling pressure of the beam tube of thickness h. Similar to the critical buckling force in Section III, this critical pressure can be obtained by demanding a *smooth* solution of Eq. (5.7) with $u_1 \equiv 0$.

The total deformation is

$$u = u_1 + u_2 = -\frac{R}{4}\frac{P_m}{p_c - p}\cos 2\varphi , \tag{5.10}$$

which demonstrates that the deformed cross section is elliptic to first order.

We next compute the stress around the beam tube cross section. First let us consider the stress in tension or compression. Substituting Eq. (5.10) into Eq. (5.3) gives the bending moment

$$M_\varphi = -\frac{\ell R^2 P_m}{4}\frac{p_c}{p_c - p}\cos 2\varphi , \tag{5.11}$$

which, according to Eq. (2.20), contributes a maximum stress of

$$\sigma_{\max}|_{\text{moment}} = \frac{6|M_\varphi|}{h^2\ell} \ . \tag{5.12}$$

To this we must add the tensile force $P_m R\ell \cos^2\varphi$ due to the Lorentz pressure and the compression force $pR\ell$ from the helium pressure. Therefore, the maximum stress at φ is

$$\sigma_\varphi = |p - P_m \cos^2\varphi|\frac{R}{h} + \frac{3P_m}{2}\frac{R^2}{h^2}\frac{p_c}{p_c - p}|\cos 2\varphi| \ . \tag{5.13}$$

The negative sign in the first term reminds us of the pressing inward of the helium pressure and pulling outward of the Lorentz pressure. We see that the contribution of the bending moment attains a maximum at the vertical point V ($\varphi = 0$) and the horizontal point H ($\varphi = \pi/2$) and vanishes at the $\pi/4$ points (Fig. 5a). We therefore expect the stress to be higher at these two points. When $p > P_m/2$,

$$\sigma_H = \frac{pR}{h} + \frac{3P_m}{2}\frac{R^2}{h^2}\frac{p_c}{p_c - p} \tag{5.14}$$

is bigger than σ_V. However, when $p < P_m/2$,

$$\sigma_V = (P_m - p)\frac{R}{h} + \frac{3P_m}{2}\frac{R^2}{h^2}\frac{p_c}{p_c - p} \tag{5.15}$$

is bigger than σ_H. It is also easy to show that both points H and V are points of local maxima. This is because if we deviate from either point by a small amount, both the tensile force and the bending moment become smaller. Given an equatorial Lorentz pressure P_m, the yield helium pressure can now be solved directly from Eqs. (5.14) and (5.15) by equating either σ_H or σ_V to the yield stress in tension or compression σ_{yp}. When the helium pressure is zero, from Eq. (5.15), we recover the yield Lorentz pressure

$$(P_m)_{yp} = \frac{\sigma_{yp}}{\frac{R}{h}\left(1 + \frac{3R}{2h}\right)} \tag{5.16}$$

that will break the point V as given by Eq. (4.11). On the other hand, if the Lorentz pressure is absent, $P_m = 0$, the tube can yield at any point since the problem becomes cylindrically symmetric again. Taking Eq. (5.14), we find that the yield helium pressure p_{yp} satisfies the quadratic equation

$$\left(\frac{p_{yp}}{p_c}\right)^2 - \left(\frac{h\sigma_{yp}}{Rp_c} + 1\right)\frac{p_{yp}}{p_c} + \frac{h\sigma_{yp}}{Rp_c} = 0 \ , \tag{5.17}$$

giving the solution

$$p_{yp} = p_c \quad \text{or} \quad \frac{h\sigma_{yp}}{R} \tag{5.18}$$

depending on which is smaller. The first solution is the critical buckling pressure while the second solution is the pressure required to produce a tensile stress that exceeds the yield stress. This second solution will arrive first when

$$\frac{4\sigma_{yp}}{E'}\frac{R^2}{h^2} < 1 \ , \tag{5.19}$$

which is the situation of a small yield stress σ_{yp} or a thick tube wall.

In addition to the shearing force due to the Lorentz pressure, there is also a shearing force due to helium pressure. This shearing force is largest at points A, B, C, and D in Fig. 5a where the angles of deformation are largest. The tangent of these angles is given by

$$\frac{du}{Rd\varphi} = -\frac{2u_m}{R} \ , \tag{5.20}$$

where

$$u_m = \frac{R}{4}\frac{P_m}{p_c - p} \tag{5.21}$$

is the maximum deformation obtained from solution (5.10). Since $u_m/R \ll 1$, the maximum helium shear stress is therefore

$$S_{He} \simeq \frac{pR\ell}{h\ell}\frac{2u_m}{R} = \frac{2u_m p}{h} \ , \tag{5.22}$$

which is of opposite sign with respect to the Lorentz shear stress S_L given by Eq. (4.12). In order to avoid elastic shear failure, we must have

$$\left|\frac{P_m R}{2h} - \frac{P_m R}{2h}\frac{p}{p_c - p}\right| < \tau_{yp} \ . \tag{5.23}$$

We are going to show that this shear failure limit is always less stringent than the tensile failure limit. For convenience, let us write everything in terms of the critical buckling pressure p_c:

$$P_m \to \frac{P_m}{p_c} \ , \qquad p \to \frac{p}{p_c} \ , \qquad \tau_{yp} \to \frac{\tau_{yp}}{p_c} \ , \qquad \sigma_{yp} \to \frac{\sigma_{yp}}{p_c} \ , \tag{5.24}$$

and also $m \to R/h$. Then from Eq. (5.23), the elastic shear yield-point Lorentz pressure for any helium pressure p is

$$(P_m|_{\rm sh})_{yp} = \frac{1-p}{|1-2p|}\frac{2\tau_{yp}}{m} \ . \tag{5.25}$$

The vanishing of the denominator $|1-2p|$ occurs when the Lorentz shear just balances the helium shear. Since $|1-2p| \leq 1$, Eq. (5.25) implies

$$(P_m|_{\rm sh})_{yp} > (1-p)\frac{2\tau_{yp}}{m} \ . \tag{5.26}$$

On the other hand, the elastic tensile yield-point Lorentz pressure is

$$(P_m|_{\rm ten})_{yp} \leq (1-p)\left(\frac{2\sigma_{yp}}{3m^2} - \frac{2p}{3m}\right) \ , \tag{5.27}$$

where use has been made of Eqs. (5.14) and (5.15). Comparing Eqs. (5.26) and (5.27), it is clear that

$$(P_m|_{\rm sh})_{yp} > (P_m|_{\rm ten})_{yp}$$

for any helium pressure p provided that

$$\frac{\tau_{yp}}{\sigma_{yp}} > \frac{1}{3m} = \frac{h}{3R} \ , \tag{5.28}$$

which is always true.

The SSC beam tube will be made of Nitronic 40 that has a yield stress in tension of $\sigma_{yp} = 175 \pm 35$ kpsi at 20 K, or of stainless steel with a corresponding yield stress of $\sigma_{yp} = 115 \pm 25$ kpsi. The limiting helium and Lorentz pressures are computed from Eq. (5.14) for $p > P_m/2$ and Eq. (5.15) for $p < P_m/2$ by setting the maximum stress σ_H or σ_V equal to σ_{yp}. The results are plotted in Figs. 6 and 7 with the range of uncertainty indicated by dotted curves. In each figure, the line $p = P_m/2$ is shown as dashed line, above which the yield will be at point H and below which the yield will be at point V. As a safety factor, the working yield stress is usually taken as about one half of the actual one. The limiting pressures corresponding to the working yield stress for each metal have also been included in the figures.

These limiting curves are very sensitive to the ratio m of the tube radius R to the tube thickness h. The critical buckling pressure p_c varies as m^{-3} while the yield Lorentz pressure is roughly proportional to m^{-2} as depicted in Eqs. (5.9) and (5.16) respectively. If, for example, the tube radius is increased by a factor of two or the tube thickness is decreased by a factor of two so that m is doubled, the $\sigma_{yp} = 175$ kpsi limiting curve in Fig. 6 becomes very much more restrictive. It starts off from helium pressure $p = p_c \sim 15$ atm, a factor of 8 smaller and ends at Lorentz pressure $P_m \sim 50$ psi, a factor of 4 smaller.

In order to obtain yield pressures greater than those shown in Figs. 6 and 7, we increase the tube thickness from 1 mm to 1.5 mm. The new results for the two types of metal are shown in Figs. 8 and 9. In Fig. 9, we see that when the yield stress

in tension is $\sigma_{yp} = 57.5$ kpsi or $\sigma_{yp} = 45.0$ kpsi, the stability curves do not fall off from the critical buckling pressure $p_c = 408.5$ atm, but rather they fall off from their respective $\sigma_{yp}h/R$ values because the condition (5.19) has been met.

The time after a quench when the Lorentz pressure is maximum has been calculated by Meuser.[3] For a copper layer of thickness in the range from 2 to 6 mils, the maximum occurs roughly when the dipole flux density B is about 5 T, the rate of change of flux density $\dot{B}$ is about -23 T/sec, and the beam tube temperature is about 20 K. Taking a conservative copper conductivity of $\sigma_1 = 6.5 \times 10^9$ $(\Omega\text{-m})^{-1}$, a copper layer of $t_1 = 2$ mil, and a beam tube radius of 1.66 cm leads to an equatorial Lorentz pressure P_m of about 91 psi. According to Fig. 6 for a tube thickness of 1 mm, the helium pressure cannot be bigger than about 60 atm to be on the safe side. However, if the copper layer has a thickness of 4 mils, P_m becomes about 182 psi and the allowable helium pressure is less than 10 atm.

VI. BEAM-TUBE TORQUE LIMITATIONS

If the copper layer on the inner surface of the bore tube of the SSC dipoles is not uniform in thickness, the Lorentz forces due to the currents induced in the copper by the collapsing magnetic field during a quench of the magnet can produce a torque tending to twist the tube about its axis.[4] If, for example, the copper thickness varies with the polar angle φ as,

$$t(\varphi) = t_1(1 + \epsilon \sin 2\varphi) \ , \tag{6.1}$$

from Fig. 1a and Eq. (4.2), the torque for a length ℓ of the tube is

$$\tau = 4 \int_0^{\frac{\pi}{2}} d\varphi P_m R^2 \ell \epsilon \sin 2\varphi \sin\varphi \cos\varphi \ , \tag{6.2}$$

where P_m is the Lorentz pressure at the equator. Then the Lorentz torque per unit length per radius squared is

$$\frac{\tau}{\ell R^2} = \frac{1}{2} \pi \epsilon P_m \ . \tag{6.3}$$

This torque is resisted by the plastic keys attached to the top and bottom of the bore-tube correction-winding assembly (Fig. 10). These keys fit into slots at the centers of the poles of the magnetic collars. The keys are 3 in. in length and occur every 18 in down the length of the bore tube. In cross section, the keys are 0.131-0.132 in. in width where they fit into the 0.132-0.134 in. slots in the collars and 0.200 in. in width at the base where they are glued to the Kapton outer layers of the correction-winding assembly. The keys are located relative to the bore tube

by 0.080 in. diameter plastic pins that are attached to the bore tube and fit into corresponding holes in the keys. The bore-tube winding assembly is glued to the bore tube and also tightly strapped to the bore tube, so that it can transmit any torque in the bore tube out to the collar. The weak point in this chain is the plastic key.

A reaction force F will be acting on the key by the collar at a distance d above the copper layer on the bore tube. Then this force is given by

$$\tau = 2F(R + d) \ , \tag{6.4}$$

where d is the height of the key from the base up to the point where F is acting ($\sim$ 3 mm) plus the thickness of the wrapping ($\sim$ 1 mm).

Suppose that the elastic limit is met at a cross section of the key at a distance d' from the point where F acts. If the shear yield point τ_{yp} is exceeded, we have

$$\frac{F}{ab} = \tau_{yp} \ . \tag{6.5}$$

If the tensile yield point σ_{yp} is exceeded, according to Eq. (2.20) we have

$$\frac{6Fd'}{a^2 b} = \sigma_{yp} \ , \tag{6.6}$$

where a and b are the width and length of the key at the cross section where the failure occurs.

The ratio of the yield shear force $F_{\rm sh}$ to the yield tensile force $F_{\rm ten}$ is

$$\frac{F_{\rm sh}}{F_{\rm ten}} = \frac{6d'}{a}\frac{\tau_{yp}}{\sigma_{yp}} \ . \tag{6.7}$$

If the failure is at the base, $a = 0.2$ in and $d' = 3$ mm. However, if the failure is midway from the base, $a = 0.131$ in and $d' = 1.5$ mm. Then

$$\frac{F_{\rm sh}}{F_{\rm ten}} = \begin{cases} 3.54\dfrac{\tau_{yp}}{\sigma_{yp}} & \text{base} \\[2ex] 2.70\dfrac{\tau_{yp}}{\sigma_{yp}} & \text{midway} \end{cases} \tag{6.8}$$

Since τ_{yp}/σ_{yp} varies between 0.5 to 0.7, we can conclude that the failure in a cross section is more likely due to tensile stress than to shear stress.

We will estimate the limiting torque on the bore tube when elastic failure occurs in three ways:

1. Experimental limit

Skaritka[5] has measured, at room temperature, the torque τ_d at which the plastic keys deform, the result being about 40 to 50 ft-lbs. The corresponding bore-tube yield torque per unit length per radius squared is

$$\frac{\tau}{\ell R^2} = \frac{\tau_d}{\ell R^2} = 62.3 \text{ to } 77.9 \text{ psi} , \tag{6.9}$$

where ℓ has been taken as 18 in., the distance between the keys down the length of the bore tube. Skaritka estimates that these materials are two to three times stronger at cryogenic temperatures and plans to repeat the experiment at helium temperature.

2. Shear failure

Skaritka attributes a cryogenic shear strength τ_{yp} to the key material in the range of 3000 to 4000 psi from measurements by Naseem Munshi[6] for the LBL magnet group. We apply such a shearing stress to a cross section of the key at midway where the area $a \times b = 0.131$ in $\times 3$ in is smallest and is therefore weakest. Using Eqs. (6.4) and (6.5), the corresponding yield torque per unit length per radius squared is

$$\frac{\tau}{\ell R^2} = \frac{2ab(R+d)}{\ell R^2}\tau_{yp} = 246 \text{ to } 328 \text{ psi} . \tag{6.10}$$

3. Tension failure

Assuming a shear yield strength to a tensile yield strength of about 0.7, we can estimate the tensile yield strength of the key material σ_{yp} to be in the range of 4290 to 5710 psi. If the failure is at the base of the key, $a = 0.2$ in. and $d' = 3$ mm. Then, applying Eqs. (6.4) and (6.6), the corresponding yield torque per unit length per radius squared is

$$\frac{\tau}{\ell R^2} = \frac{a^2 b(R+d)}{3\ell R^2 d'}\sigma_{yp} = 150 \text{ to } 204 \text{ psi} . \tag{6.11}$$

If the failure is at the midplane, $a = 0.131$ in. and $d' = 1.5$ mm. Then we have

$$\frac{\tau}{\ell R^2} = 129 \text{ to } 175 \text{ psi} . \tag{6.12}$$

From the above three estimates, we learn that the key will meet with a tensile elastic failure before a shear failure, as we mentioned above. Also the tensile failure will occur at the midplane rather than the base of the key. The results of the experiment in the first estimate do not disagree with the results in the third estimate because the material of the key is expected to be stronger at cryogenic temperatures.

If as a safety factor, the working yield stress is again taken as one half the actual one, then the allowable torque $\tau/\ell R^2$ is about 65 psi. If we take the equatorial Lorentz pressure P_m as about 45.5 psi per mil of copper layer thickness, as estimated in Section V, Eq. (6.3) leads to

$$t_1 \epsilon \approx 0.89 \text{ mil} . \tag{6.13}$$

This implies that for a copper thickness of $t_1 = 2$ mil, the thickness variation ϵ as defined in Eq. (6.1) must be less than 45%. If the layer thickness is $t_1 = 4$ mil, the variation ϵ must be less than 22%.

The authors would like to thank Dr. R. B. Meuser for useful discussions, meaningful comments, and his checking of some of the formulas.

APPENDIX A

During a quench of the magnet, the dipole field drops at a rate $\dot{B}$ and an emf $\mathcal{E}$ will be induced in the copper layer on the beam tube. According to Faraday's law, for a length ℓ at polar angle φ,

$$\mathcal{E}(\varphi)\ell = \dot{B}\ell R \sin\varphi \ . \tag{A.1}$$

The eddy current density will be

$$J(\varphi) = \sigma_1 \mathcal{E}(\varphi) \ , \tag{A.2}$$

where σ_1 is the conductivity of copper. Being inside a magnetic flux density B, the Lorentz force pulling horizontally outward on a strip of copper subtending an angle $d\varphi$ is

$$\begin{aligned} dF(\varphi) &= \int_{\text{volume}} |BJ| d^3v \\ &= \sigma_1 |B\dot{B}| t_1 \ell R^2 \sin\varphi d\varphi \ , \end{aligned} \tag{A.3}$$

where t_1 is the thickness of the copper layer. Since copper has a conductivity of 300 to 3000 times that of Nitronic 40 which the beam tube is made of, we have assumed that all the eddy current flows in the copper layer. The horizontally outward Lorentz pressure is therefore

$$P_L(\varphi) = \sigma_1 |B\dot{B}| t_1 R \sin\varphi \ , \tag{A.4}$$

and the maximum occurs at the equator where $\varphi = \pi/2$ or

$$P_m = \sigma_1 |B\dot{B}| t_1 R \ . \tag{A.5}$$

APPENDIX B

1. The Castigliano's Theorem

The Castigliano's theorem[7] states: If a body is deformed within the elastic limit due to the action of n *independent* external forces $F_1, \ldots, F_n$ and satisfies the following provisions: (1) the material follows Hooke's law and (2) the conditions are such that the small displacements, due to strain, do not affect the action of the external forces and are negligible in calculating the stresses, then the displacements $\delta_1, \ldots, \delta_n$ of the points of application of the forces, each measured in the direction of the corresponding force are given by

$$\delta_i = \frac{\partial W}{\partial F_i} , \tag{B.1}$$

where $W(F_1, \ldots, F_n)$ is the energy of strain of the body expressed as a function of the n external forces. All the *dependent* external forces are assumed to be doing no work here.

Before proving the theorem, let us remark first that not all of the external forces acting on the body are independent. For example, the reaction forces are dependent and are usually eliminated from the strain energy W because they do not cause any displacements at the points of action. However, all displacements are relative. Thus we can always choose whichever forces as independent to suit our purpose.

Second, the provisions (1) and (2) imply that the displacements are linear functions of the external forces, or

$$\delta_i = \sum_{j=1}^{n} K_{ij} F_j , \tag{B.2}$$

where the matrix K is independent of the forces F_j. We want to point out that provision (1) alone does not warrant these linear relations. Problems such as the bending of bars by lateral forces with simultaneous axial tension or compression do not satisfy provision (2) and are excluded from this discussion.

To proceed to the proof, let us first compute the strain energy. Suppose we start with all external forces equal to zero and increase only F_1 slowly to its full value. The strain energy is equal to the work done by F_1, or using Eq. (B.2),

$$W_1 = \int_0^{F_1} \delta_1 dF_1' = \frac{1}{2} K_{11} F_1^2 . \tag{B.3}$$

Next we hold F_1 fixed and increase F_2 slowly to its full value ($F_3, \ldots, F_n$ remain zero), the additional strain energy is

$$W_2' = \int_0^{F_2} \delta_2 dF_2'$$

$$
\begin{aligned}
&= \int_0^{F_2} (K_{21}F_1 + K_{22}F_2')dF_2' \\
&= K_{21}F_2F_1 + \frac{1}{2}K_{22}F_2^2 \ . \qquad \text{(B.4)}
\end{aligned}
$$

Therefore the strain energy due to F_1 and F_2 is

$$
W_2 = \frac{1}{2}K_{11}F_1^2 + K_{21}F_2F_1 + \frac{1}{2}K_{22}F_2^2 \ . \qquad \text{(B.5)}
$$

However, we will get exactly the same strain energy if we apply F_2 first and then F_1. Obviously this implies that $K_{21} = K_{12}$ or the matrix K is symmetric. Then, it is easy to write the strain energy due to all the n external forces as

$$
W(F_1, \ldots, F_n) = \sum_{i,j=1}^{n} \frac{1}{2}K_{ij}F_iF_j \ . \qquad \text{(B.6)}
$$

Differentiation with respect to F_i gives

$$
\frac{\partial W}{\partial F_i} = \sum_{j=1}^{n} K_{ij}F_j = \delta_i \ , \qquad \text{(B.7)}
$$

which is the Castigliano's theorem.

Instead of external force F_i and displacement δ_i, the Castigliano's theorem can be trivially extended to include external couple M_i and the angular displacement φ_i at the point where the couple acts.

2. Applications

Here we apply the Castigliano's theorem to the deformation of the beam pipe due to Lorentz pressure. We will compute the bending moment M_0 at the point V in Fig. 1b and then the deformations at V and H.

Consider an infinitesimal section $ds = Rd\varphi$ on the beam tube. The angular displacement $d\bar{\varphi}$ due to a bending moment M_φ at this section is

$$
d\bar{\varphi} = \frac{M_\varphi R d\varphi}{E'I} \ , \qquad \text{(B.8)}
$$

according to the basic equation for deformation of Eq. (2.3) or (2.18). Here, $Rd\varphi/E'I$ is just the corresponding K of Eq. (B.1). Thus, the strain energy in any section of the beam tube is given by

$$
W = \int \frac{M_\varphi^2 R}{2E'I} d\varphi \ , \qquad \text{(B.9)}
$$

where the integration is performed over the section of the tube under consideration. In above, the contributions of tensile and shear energies have been neglected because they are a factor $(h/R)^2$ smaller, where h is the tube thickness.

To obtain the deformation at V and H, we add two fictitious forces F_V and F_H at V and H respectively as shown in Fig. 11. The force F_V is split into two halves on both sides of the point V to preserve the symmetry of the point V. These forces will be put to zero at the end of the computation.

Consider the section VC. Taking moment about C, the bending moment at C or at angle φ is

$$\begin{aligned} M_\varphi &= M_0 - \int_0^\varphi \frac{F_t}{2} \sin\theta R(\cos\theta - \cos\varphi) d\theta + \frac{F_V}{2} R \sin\varphi + \frac{F_t + F_H}{2} R(1 - \cos\varphi) \\ &= M_0 + \frac{F_t}{4} R \sin^2\varphi + \frac{F_V}{2} R \sin\varphi + \frac{F_H}{2} R(1 - \cos\varphi) \ , \end{aligned} \tag{B.10}$$

where M_0 is the couple supporting the section at V, the second term on the right side of the first line is due to the Lorentz force, the third term is the moment due to the vertical fictitious force at V, and the last term is the moment of the horizontal tensile force at V supporting the section VC. Note that this expression is exactly the same as Eq. (4.3) if we set $F_V = F_H = 0$.

Now consider the section VH which is supported by the independent distributed Lorentz force on the arc, $F_V/2$ and $(F_t + F_H)/2$ at V as well as the couple M_0 at V. The strain energy is

$$W_{VH} = \int_0^{\frac{\pi}{2}} \frac{M_\varphi^2 R}{2E'I} d\varphi \ . \tag{B.11}$$

By symmetry, it is evident that there is no angular displacement at the point V. Therefore, applying the Castigliano's theorem,

$$\frac{\partial W_{VH}}{\partial M_0} = 0 \ , \tag{B.12}$$

we get

$$\int_0^{\frac{\pi}{2}} M_\varphi d\varphi = 0 \ , \tag{B.13}$$

or

$$M_0 = -\frac{F_t R}{8} - \frac{F_V R}{\pi} - \frac{F_H R}{2}\left(1 - \frac{2}{\pi}\right) \ . \tag{B.14}$$

which becomes $M_0 = F_t R/8$ in the limit $F_V = F_H = 0$ as expected in Section IV. Using Eqs. (B.10) and (B.14), the bending moment at any point in the beam tube can now be written as

$$M_\varphi = -\frac{F_t}{8} R \cos 2\varphi - \frac{F_V}{2} R\left(\frac{2}{\pi} - \sin\varphi\right) + \frac{F_H}{2} R\left(\frac{2}{\pi} - \cos\varphi\right) \ . \tag{B.15}$$

We next consider the tube as a whole, which is supported by the independent distributed Lorentz forces, F_V at V and F_H at H. The strain energy energy is

$$W = 4\int_0^{\frac{\pi}{2}} \frac{M_\varphi^2 R}{2E'I} d\varphi \ . \tag{B.16}$$

The displacements at V and H are given respectively by

$$\delta_V = \left.\frac{\partial W}{\partial F_V}\right|_{F_V=F_H=0} = \frac{F_t R^3}{12E'I} \ , \tag{B.17}$$

$$\delta_H = \left.\frac{\partial W}{\partial F_H}\right|_{F_V=F_H=0} = \frac{F_t R^3}{12E'I} \ . \tag{B.18}$$

In the derivation, we have made the assumption that the point opposite to V and the point opposite to H do not move. Therefore the displacements δ_V and δ_H are the total contraction and extension of the *diameter* of the beam tube. We see that the results agree with the deformations obtained in Eq. (4.7).

One may raise the question that as we let the fictitious forces go to zero, why don't their corresponding displacements δ_V and δ_H go to zero also. This apparent paradox is answered by the fact that the matrix K in Eq. (B.1) is not diagonal. For example, the displacement δ_V does not depends only on F_V. It also depends on the helium pressure F_H, as well as the Lorentz force distribution.

REFERENCES

1. S. Timoshenko, *Strength of Materials,* 3rd Ed., 1957, Van Nostrand.
2. O. Domke, *Bautechnik,* Vol. 4, p.747, 1926.
3. R. Meuser, *Eddy-Current Forces on the dipole Bore Tube During a Quench,* SSC Report SSC-N-447, 1988.
4. A. Chao, *More on Copper Coating Considerations,* SSC Report SSC-N-434, 1987.
5. Skaritka, private communication.
6. N. Munshi, private communication.
7. What we give here is our interpretation and proof of the Castigliano's theorem. For Castigliano's original proof, see A. Castigliano, *Nuova teoria intorno dell' equilibrio dei sistemi elastici,* Atti Acc. Sci. Torino, 1975.

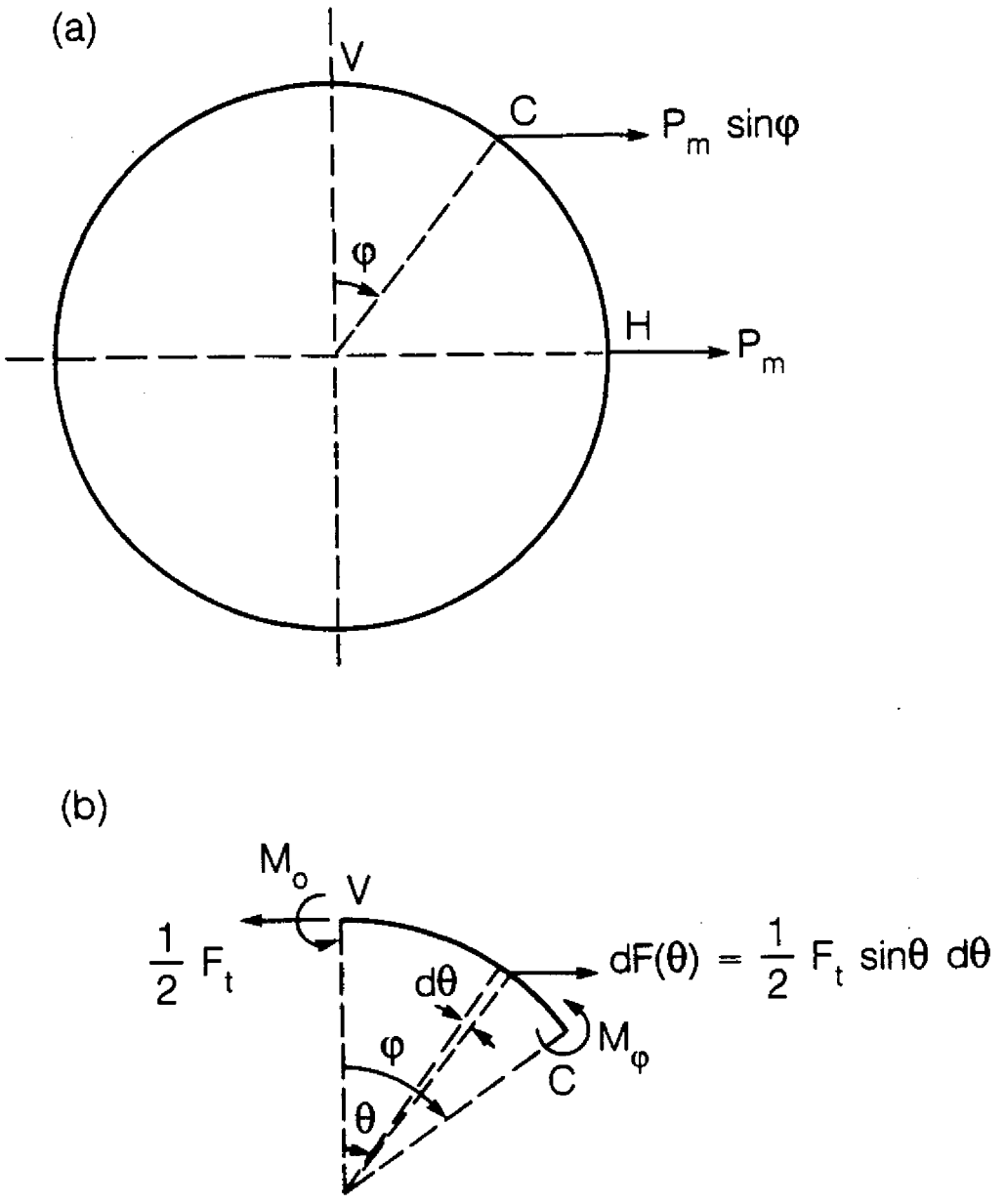

Fig. 1 (a) The pressure produced by the horizontal Lorentz forces acting on the eddy currents in the thin copper layer varies sinusoidally with the polar angle φ, the angle with respect to the direction of the dipole magnetic field.

(*b*) The bending moment M_φ in the beam tube at φ is equal to the sum of the moment M_0 at V plus the moments due to the tension force $\frac{1}{2} F_t$ at V plus the integral moment due to the Lorentz forces.

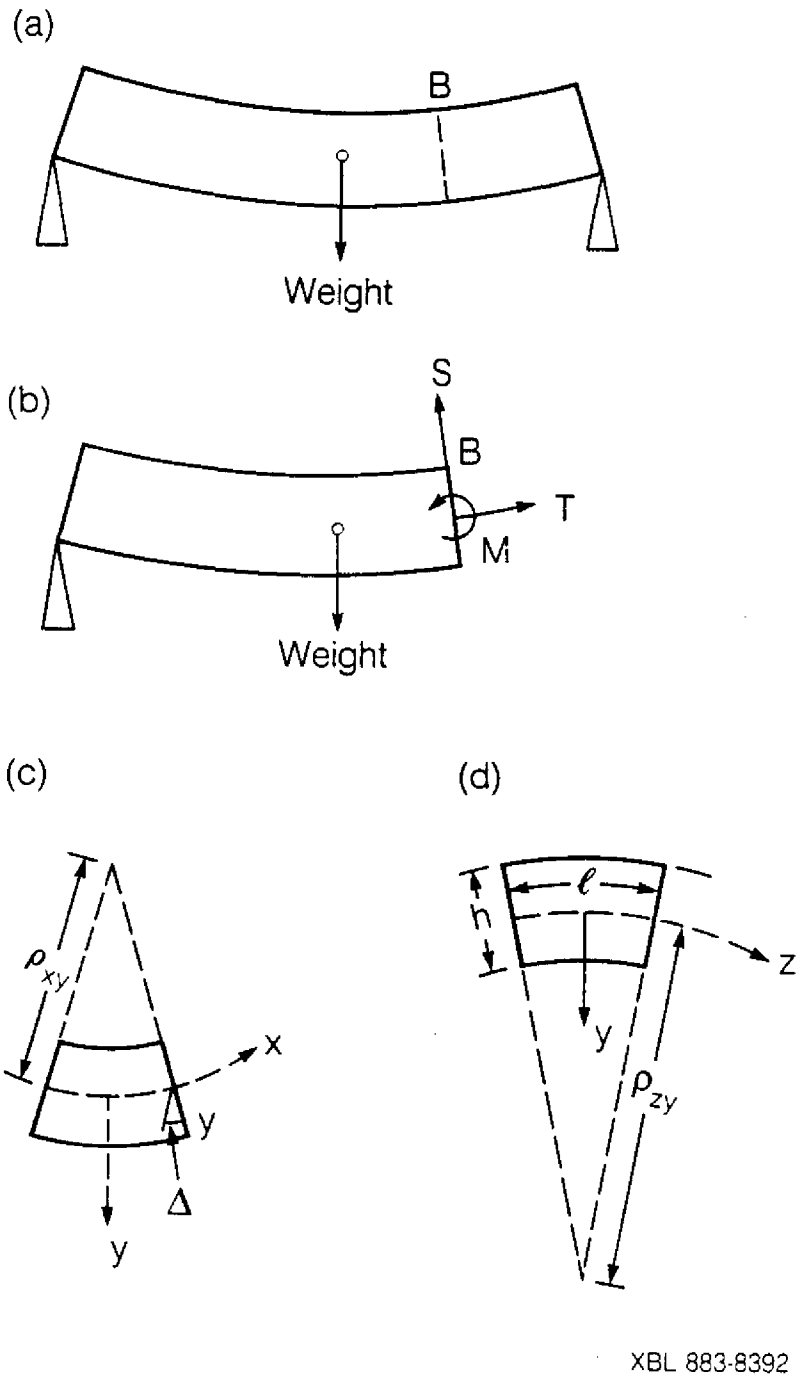

Fig. 2 (a) Uniform massive beam supported at its ends.

(*b*) Bending moment M, tensile force T, and shearing force S at arbitrary section B of the beam.

(*c*) y-x cross section of the beam. The x-direction is along the neutral axis of the beam, and the y-direction is down, the curvature of the beam puts the top of the beam in compression and the bottom in tension.

(*d*) y-z cross section of the beam. The z-direction is the other transverse direction. Because of the Poisson's ratio effect, the top width of the beam is increased and the bottom width decreased.

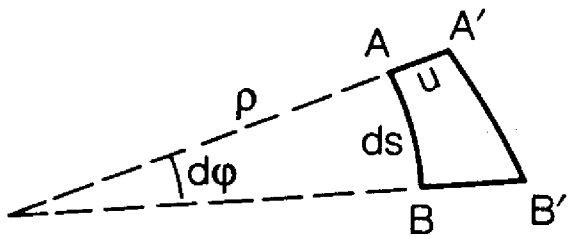

XBL 883-8396

Fig. 3 A differential section ds of the neutral axis AB is deformed to the position $A'B'$, u being the displacement.

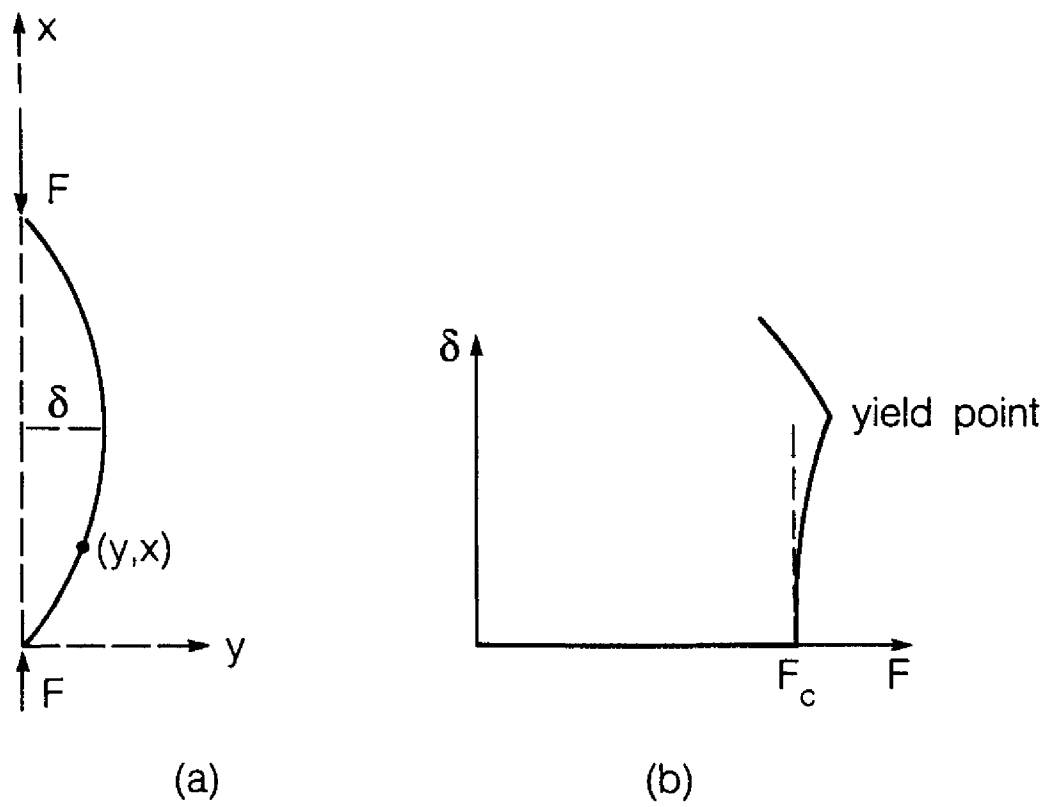

XBL 883-8398

Fig. 4 (a) The vertical force F acting on a thin rod tends to produce buckling. The lowest mode of buckling is illustrated.

(*b*) The maximum displacement δ is zero up to critical force F_c and then increases rapidly up to the yield point, beyond which the material deforms inelastically.

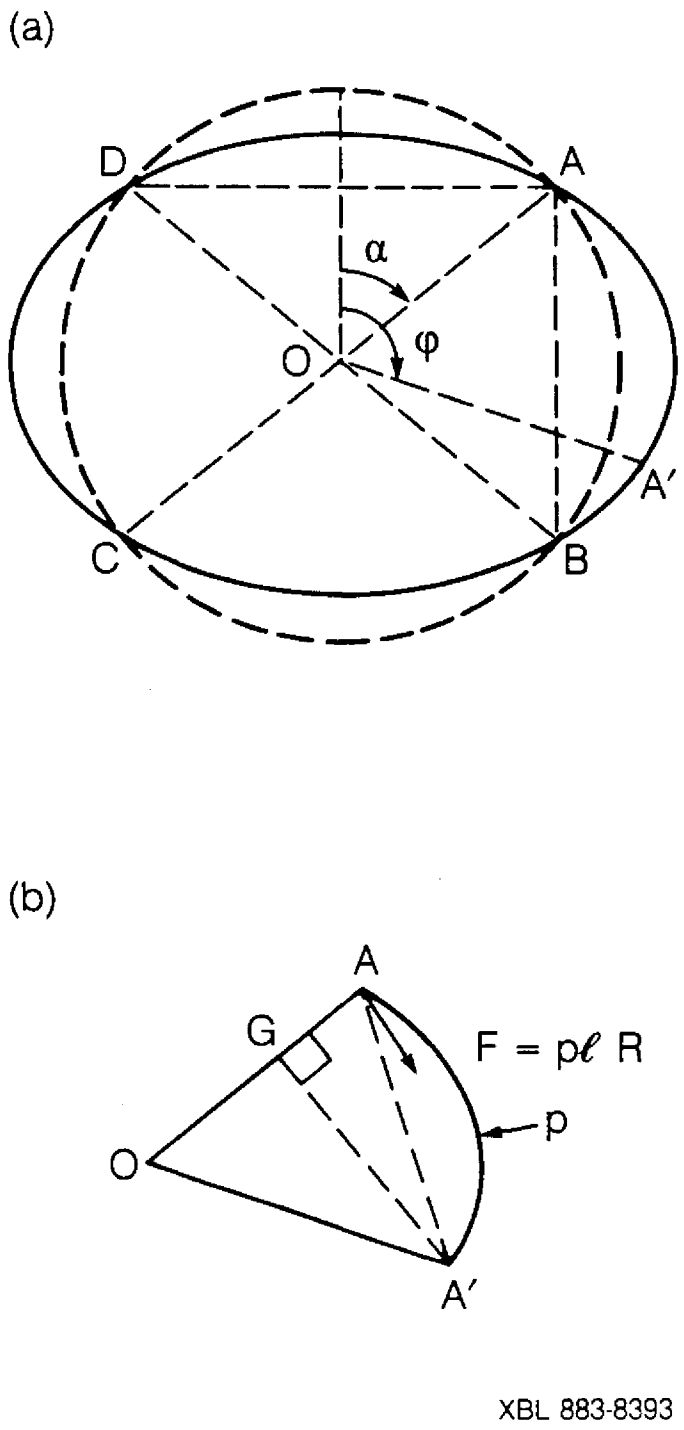

Fig. 5 (a) Because of the horizontal Lorentz forces, the round beam tube (dashed circle) is deformed into an ellipse-like shape. At the four points A, B, C, D, the radius of curvature is unchanged and therefore the bending moment vanishes.

(*b*) Section AA' of the elliptical structure. p is the external pressure due to the helium. F is the total force at end A due to the helium and is tangential to the circle.

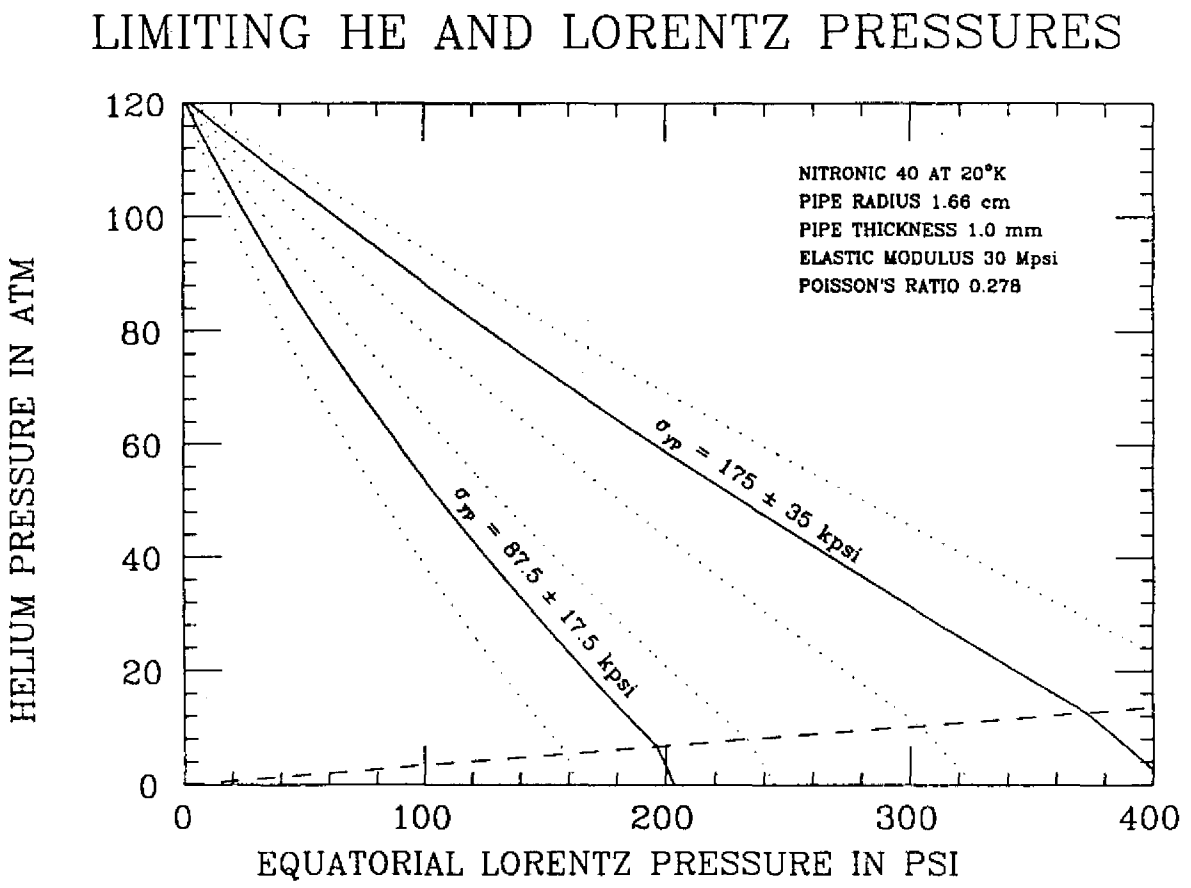

Fig. 6 The limiting helium and Lorentz pressures corresponding to the expected Nitronic 40 yield-point stress of 175 kpsi at 20°K (upper curves). The dotted curves correspond to the uncertainty of ±35 kpsi in σ_{yp}. The lower curves result if a safety factor of two in σ_{yp} is applied. Beam tube radius is 1.66 cm and wall thickness is 1.0 mm.

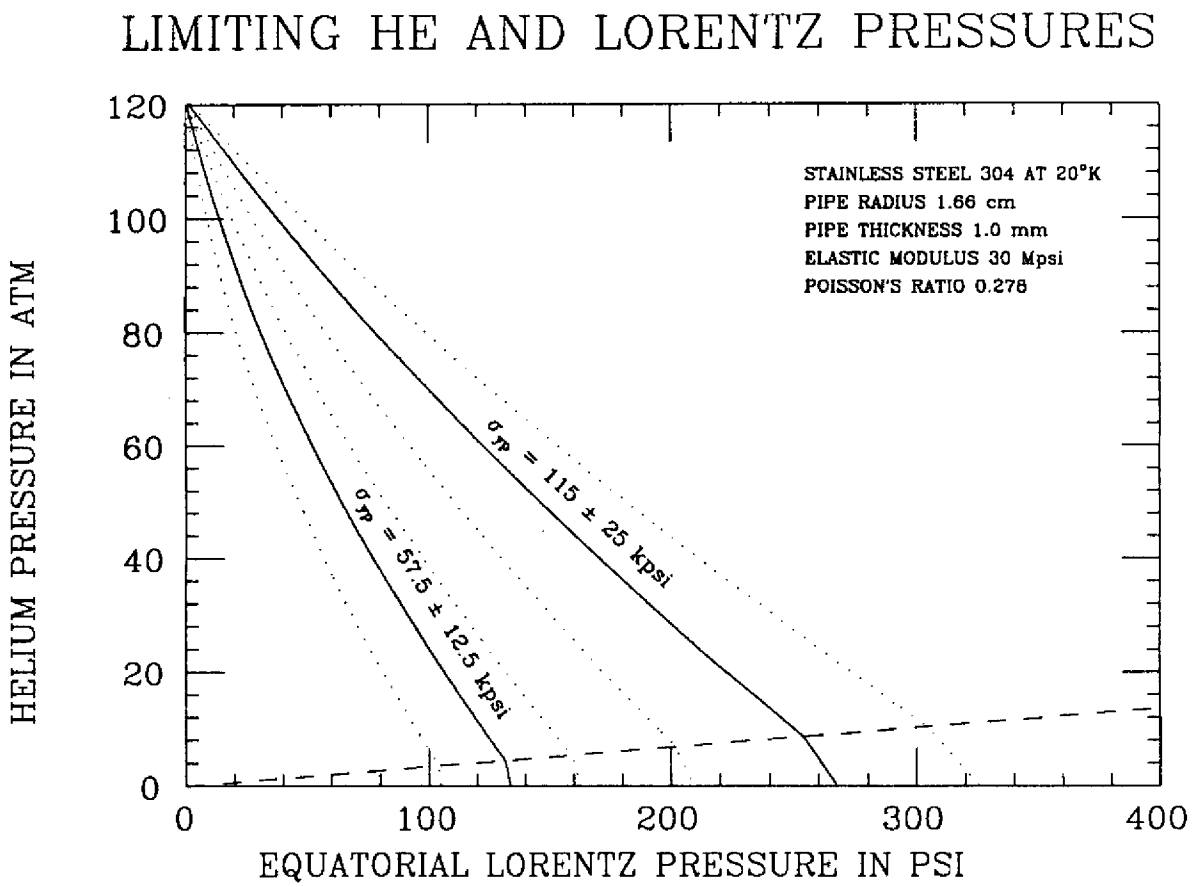

Fig. 7 The limiting helium and Lorentz pressures corresponding to the expected stainless steel yield-point stress of 115 ± 25 kpsi (upper curves). The lower curves result if a safety factor of two in σ_{yp} is applied. Beam tube radius is 1.66 cm and wall thickness is 1.0 mm.

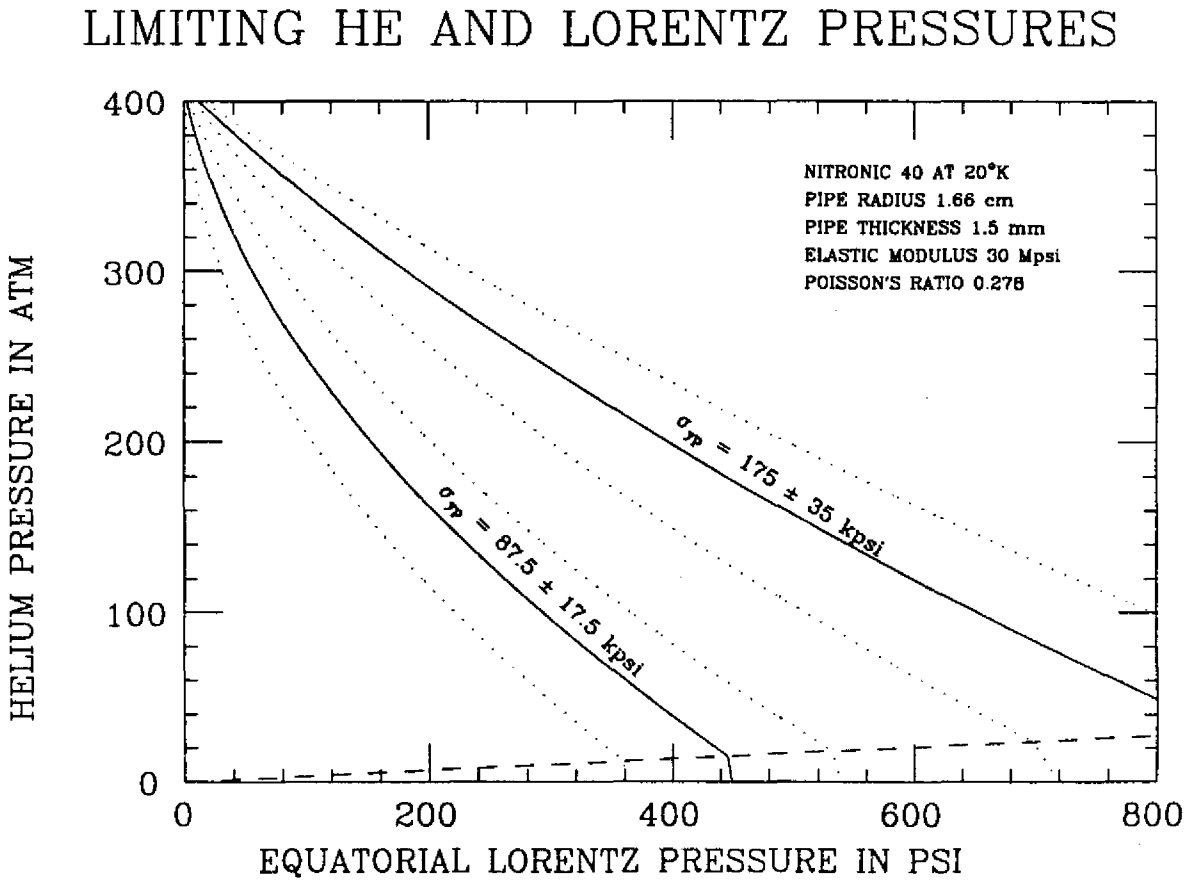

Fig. 8 The limiting helium and Lorentz pressures if the thickness of the Nitronic 40 beam tube (Fig. 6) is increased to 1.5 mm.

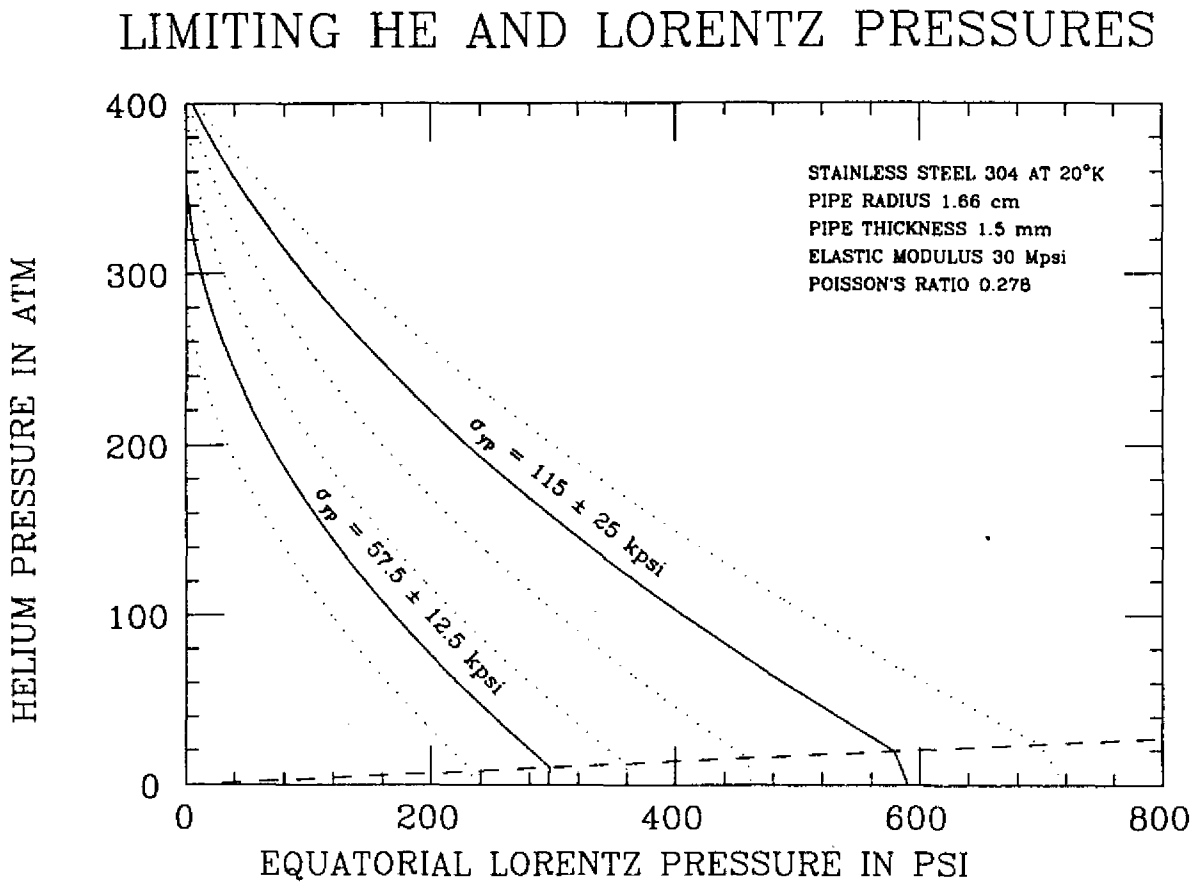

Fig. 9 The limiting helium and Lorentz pressures if the thickness of the stainless steel beam tube (Fig. 7) is increased to 1.5 mm. Note for the cases $\sigma_{yp} = 57.5$ and 45 kpsi that the helium pressures at zero Lorentz pressure occur at $\sigma_{yp}h/R$ rather than at the critical pressure, corresponding to the condition of Eq. (5.19).

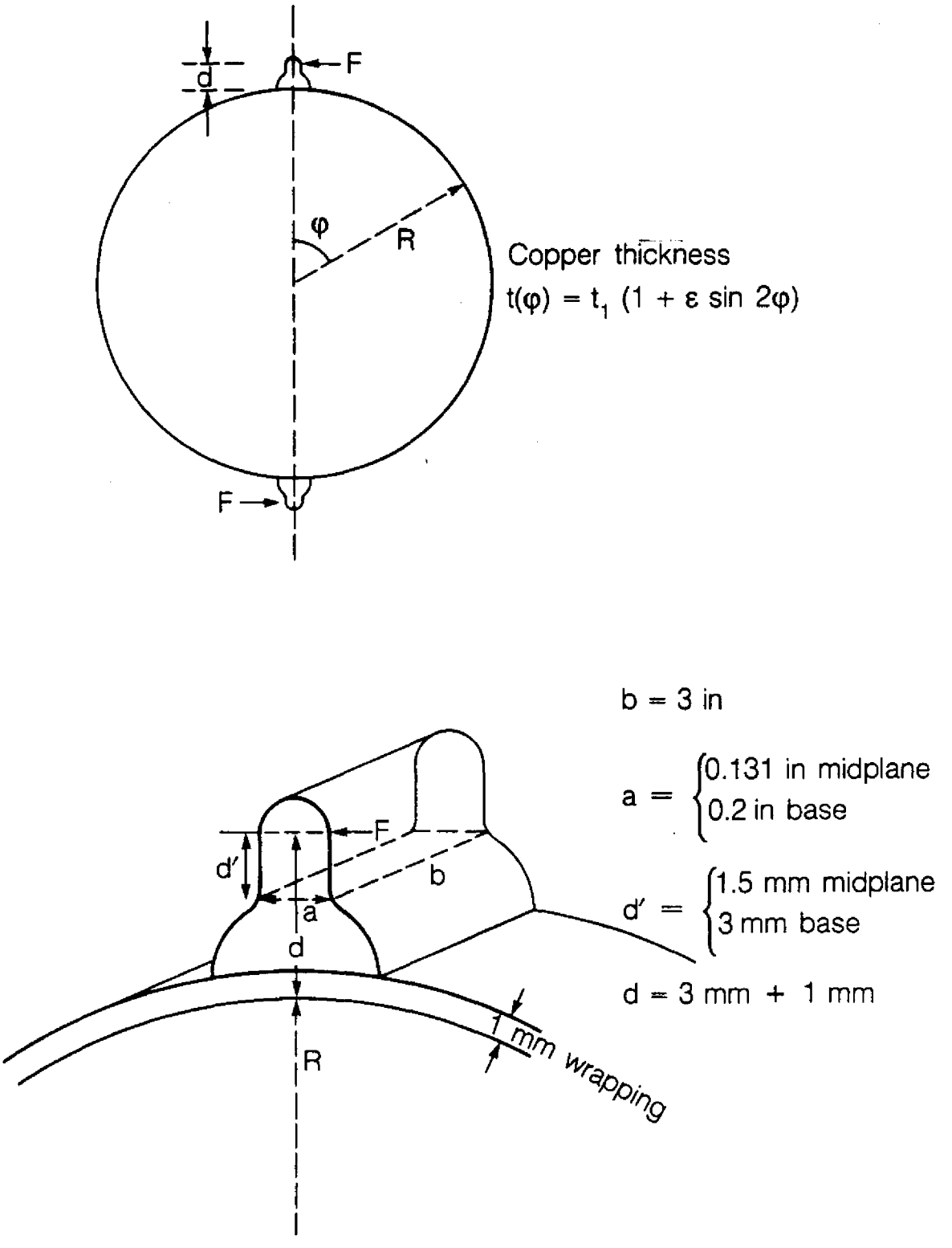

Fig. 10 Geometry of the plastic key that fixes the angular position of the beam tube with respect to the magnet collars and resists the Lorentz torque that could be produced by non-uniform copper thickness.

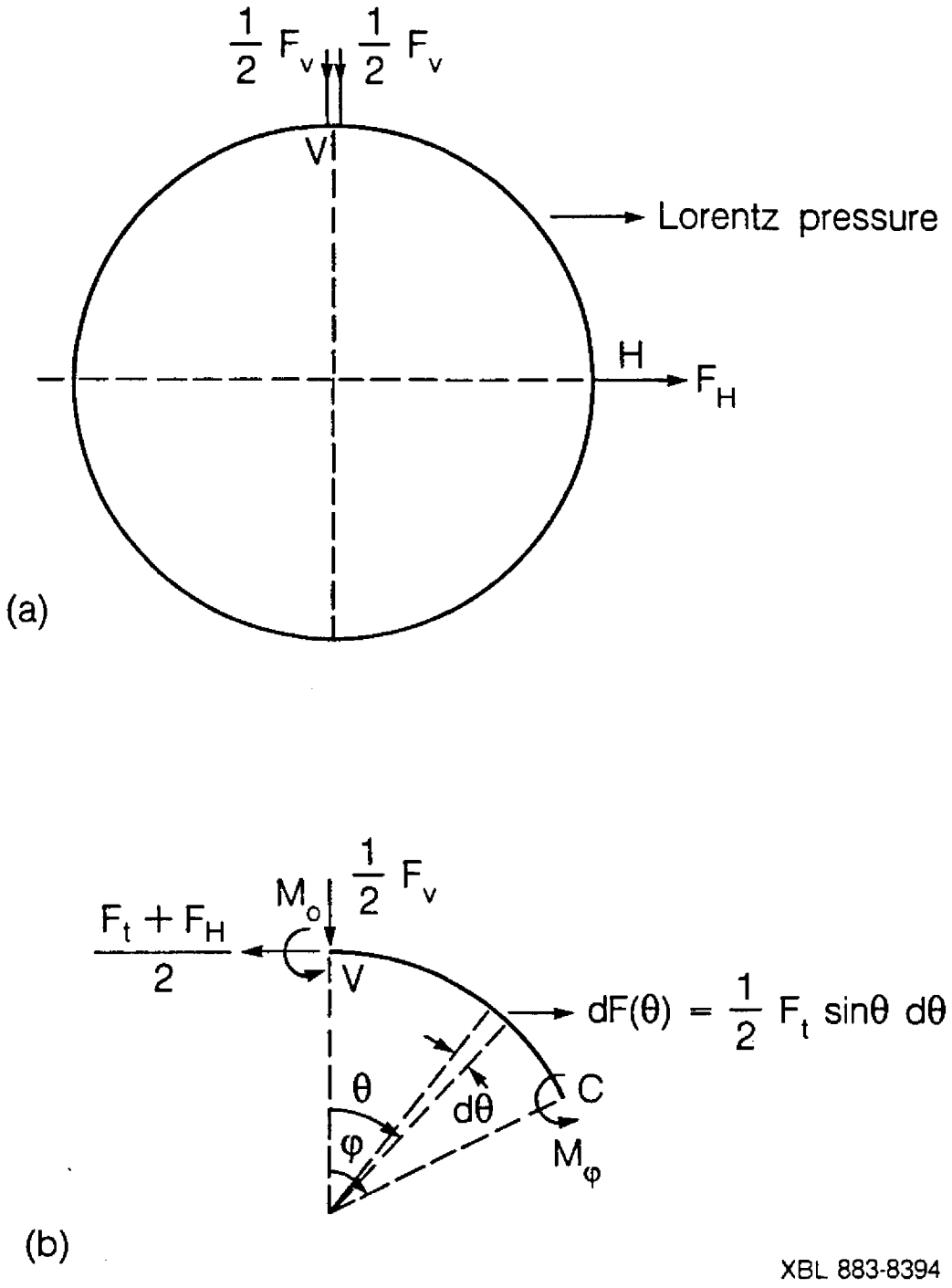

Fig. 11 (a) Geometry of the beam tube acted on by the horizontal Lorentz forces and an arbitrary vertical force F_V at V and an arbitrary horizontal force F_H at H. Same as Fig. 1 except for F_V and F_H.

(*b*) Force and moment diagram for beam-tube section VC.